Asian Research Journal of Mathematics

11(4): 1-15, 2018; Article no.ARJOM.45267
ISSN: 2456-477X

Solution of Boundary Layer and Thermal Boundary Layer Equation

Farhana Mamtaz[1], Ahammad Hossain[2*] and Nusrat Sharmin[3]

[1]Department of Mathematics, California State University, Northridge, USA.
[2]Department of Mathematics, Sonargaon University, Bangladesh.
[3]Department of Mechanical Engineering, Sonargaon University, Bangladesh.

Authors' contributions

This work was carried out in collaboration between all authors. All authors read and approved the final manuscript.

Article Information

DOI: 10.9734/ARJOM/2018/45267
Editor(s):
(1) Dr. Krasimir Yankov Yordzhev, Associate Professor, Faculty of Mathematics and Natural Sciences, South-West University, Blagoevgrad, Bulgaria.
Reviewers:
(1) Hakeem Ullah, AK University, Pakistan.
(2) N. Vishnu Ganesh, Ramakrishna Mission Vivekananda College, India.
(3) Rahim Shah, Qurtuba University of Science and IT, Pakistan.
Complete Peer review History: http://www.sciencedomain.org/review-history/27853

Short Research Article

Received: 19 September 2018
Accepted: 04 December 2018
Published: 19 December 2018

Abstract

We studied equation of continuity and boundary layer thickness. The Blasius and Falkner equations are studied in order to investigate the guess values in various boundary layer thicknesses, and Falknar-skan equations shows when velocity profile has a point of inflection in case of accelerated and decelerated. The solutions of the above mentioned equations are shown graphically. Finally, the thermal boundary layer equation has been derived from Navier-Stoke equation by boundary layer technique. Boundary Layer equation has been non-dimensionalised by using non-dimensional variable. The non-dimensional boundary layer equations are non-linear partial differential equations. These equations are solved by finite difference method. The effect on the velocity and temperature for the various parameters entering into the problems are separately discussed and shown graphically. We use Fortran Program for taking Data and for graphical representation we use TecPlot.

Keywords: Falknar-skan; navier-Stoke; blasius equation; boundary layer; thermal boundary.

**Corresponding author: E-mail: hossaina@pu.edu.bd, ahammad_dream@yahoo.com;*

1. Introduction

It all started in 1904 at the International Mathematical Congress in Heidelberg, when Ludwig Prandtl give a lecture entitled "Über Flüssigkeitsbewegungen bei sehr kleiner Reibung" (English: "On fluid flow with very little friction") [1]. He explained that the viscosity of a fluid plays a role in a (very) thin layer adjacent to the surface, which he called *"Uebergangsschicht"* or *"Grenzschicht"*. Translated into English, the latter led to term boundary layer [2,3]. The boundary layer theory plays a vital role in the variety area of engineering and scientific applications [4]. With this lecture, the understanding of fluid flow was significantly increased. For instance, D'Alembert's paradox, stating that a body placed in a potential flow does not experience a force-clearly in conflict with everyday experience-was resolved. Subsequently, it could be explained, e.g., why birds and airplanes can fly. The thus far invisible boundary layer was responsible. It plays a vital role in fluid dynamics and has become a very powerful of analysing the complex behavior of real fluids. The boundary layer flow due to a shrinking sheet is emerged as an interesting problem in fluid dynamics [5]. The shrinking sheet flows occur in some practical situations, such as, for rising shrinking balloon and it is very useful in packaging of bulk products. The drag on ships and missiles, the efficiency of compressor and turbines in jet engines, the effectiveness of air intakes for ram and turbojets and so on depend on the concept of the boundary layer and its effects on the main flow. The boundary-layer flow induced by a stretching surface has been the focus of large area during the last few decades in view of its many applications in the polymer extrusion, in a melt spinning processes, aerodynamic extrusion of plastic sheets, glass fiber production, the cooling and drying of paper and textiles, water pipes, sewer pipes, irrigation channels, blood vessels etc. The boundary-layer flow of nanofluid over a stretching sheet is a current attractive topic among the researchers [6]. With solving any equation and depending on the arguments in physical terms, the bounary layer theory is capable of explaining the difficulties encountered by ideal fluid dynamics [7]. When a real fluid (viscous fluid) flows past a stationary solid boundary, a layer of fluid which comes in contact with the boundary surface adheres to it (on account of viscosity) and condition of no slip occurs(The slip no-slip condition implies that the velocity of fluid at a solid boundary must be same as that of boundary itself). Thus, the layer of fluid which can't slip away from the boundary surface undergoes retardation for the adjacent layer of the fluid, thereby developing a small region in the immediate vicinity of the boundary surface in which the velocity of the following fluid increases rapidly from zero at the boundary surface and approaches the velocity of main stream [2]. The layer adjacent to the boundary is known as Boundary Layer. Boundary Layer is formed whenever there is relative motion between the boundary and the fluid. Since $\tau_0 = \mu\left(\frac{\partial u}{\partial y}\right)_{y=0}$ the fluid exerts a shear stress on the boundary and boundary exerts an equal and opposite force on the fluid known as the shear resistance [8].

According to boundary layer theory the extensive fluid medium around bodies moving in fluid can be divided into following two regions:

(i) A thin layer adjoining the boundary called the boundary layer where the viscous shear takes place.
(ii) A flow outside the boundary layer where the flow behaviour is quite like that of an ideal fluid and the potential theory is applicable [9].

Recntly, many authors are working on 3-D boundary layer flow. Three-dimensional boundary layer flow transition over rotating disks has been a subject of many studies. These studies are served as the foremost model problem for the subsequent investigations of the 3-D boundary layer flows over axisymmetric bodies of revolution [10]. For the Both case theoretically and experimentally, the case of a flow field structure of the laminar boundary layer flow over rotating spheres has been greatly. The flow visualisation studies led by the papers are related to the transition of the laminar boundary layer flow over rotating spheres and cones [11]. The stability and instability of the boundary layer flows on rotating spheres, spheroids, and disks. The theoretical studies of [12] related to the transition phenomena of the laminar boundary layer flow over various rotating geometries like disk, sphere and cone were carried out in such a way that the governing

laminar flow equations were first derived using some appropriate coordinate systems for each geometry. These laminar flow equations are actually a set of simultaneous 3-D nonlinear partial differential equations and are solved by using advanced numerical methods. Subsequently, the perturbation equations that govern the transition of the laminar boundary layer are derived for each body. The solutions of the laminar flow equations are then used in solving the related perturbation equations for each body [10].

The Falkner-Skan equation has been considered in the last 40 years due to its significance in the boundary layer theory. At the first time the solution of the Falkner-Skan equation has been studied numerically and solved this equation by the shooting method. A researcher Maksyn solved the Falkner-Skan equation by analytic approximation. After that, found its solution using finite differences, homotopy analysis and Fourier series to solve Falkner-Skan equation. An important case is the Blasius equation [11,4]. This problem was solved by Rosales and Valencia [13] using Fourier series. Mathematician Boyd found the solution of Falkner-Skan equation by numerical method. An enormous amount of research work has been invested in the study of nonlinear boundary value problems [4].

2. Experimental Details

The momentum thickness represents the vertical distance that the solid boundary must be displaced upward so that the ideal fluid has the same mass momentum as the real fluid.

Expression for $\delta^*$and θ using various types of velocity profiles in the boundary layer is tabulated in Table 1.

Table 1. $\delta^*$and θ for various types of velocity profiles in the boundary layer

Types of velocity distribution	Boundary layer displacement thickness, δ^*	Boundary layer momentum thickness, θ
Linear profile, $\frac{u}{U}=\frac{y}{\delta}$	$\frac{\delta}{2}$	$\frac{\delta}{6}$
Parabolic profile, $\frac{u}{U}=-\left(\frac{y}{\delta}\right)^2+2\left(\frac{y}{\delta}\right)$	$\frac{\delta}{3}$	$\frac{2}{15}\delta$
Cubic profile, $\frac{u}{U}=\frac{3}{2}\left(\frac{y}{\delta}\right)-\frac{1}{2}\left(\frac{y}{\delta}\right)^3$	$\frac{3}{8}\delta$	$\frac{39}{280}\delta$
Sin-Cos profile, $\frac{u}{U}=sin\left(\frac{\pi}{2}\frac{y}{\delta}\right)$	$\delta\left(1-\frac{2}{\pi}\right)$	$\delta\left(\frac{2}{\pi}-\frac{1}{2}\right)$
Turbulent profile, $\frac{u}{U}=\left(\frac{y}{\delta}\right)^{1/7}$	$\frac{\delta}{8}$	$\frac{7}{72}\delta$

Thus we can write,

$$2f'''(\eta)+f(\eta)f''(\eta)=0 \tag{1}$$

With boundary conditions,

$$f(\eta)=0, f'(\eta)=0 \quad \text{at} \quad \eta=0 \tag{2}$$

And

$$f'(\eta)=1 \quad \text{as} \quad \eta\to\infty \tag{3}$$

The differential equation (1) with boundary conditions (2) and (3) is known as Blasius equation [14]. Its solution is shown in Fig. 1.

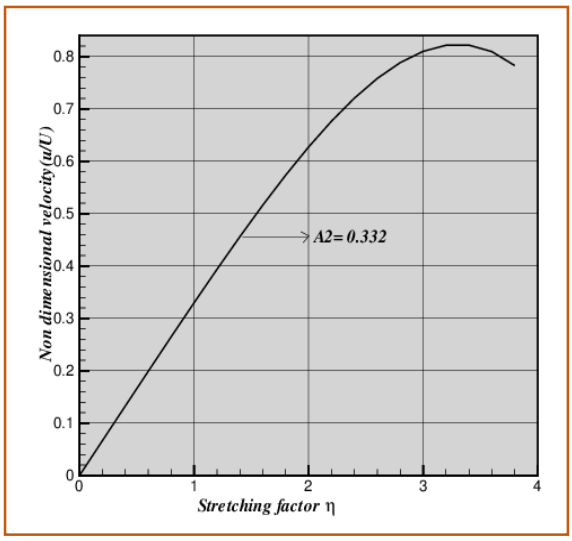

Fig. 1. Velocity distribution of Blasius equation

The solution (Blassius solution) is tabulated as follows:

Table 2. The Blassius solution

$\eta = y\sqrt{\frac{U_0}{\upsilon x}}$	$f'(\eta) = u/U$	η	$f'(\eta)$
0	0	3.6	0.9233
0.4	0.1328	4.0	0.9555
0.8	0.2647	4.4	0.9759
1.2	0.3938	4.8	0.9878
1.6	0.5168	5.0	0.9916
2.0	0.6298	5.2	0.9943
2.4	0.7290	5.6	0.9975
2.8	0.8115	6.0	0.9990
3.2	0.8767	∞	1.0000

2.1 Mathematical formulation

$$\text{For unsteady state}\ \frac{\partial T}{\partial t} + u\frac{\partial T}{\partial x} + v\frac{\partial T}{\partial y} = \frac{k}{\rho c_p}\frac{\partial^2 T}{\partial y^2} + \frac{\upsilon}{c_p}\left(\frac{\partial u}{\partial y}\right)^2 \tag{4}$$

The Navier-stokes equation in $X-$direction with boundary layer without body force due to gravity taken into account.

$$\frac{\partial u}{\partial t} + u\frac{\partial u}{\partial x} + v\frac{\partial u}{\partial y} = -g - \frac{1}{\rho}\frac{\partial p}{\partial x} + \nu\frac{\partial^2 u}{\partial y^2} \tag{5}$$

With the corresponding initial and boundary conditions are

$$\text{At } t = 0 \; U = 0, V = 0 \text{ everywhere} \tag{6}$$

$$t > 0$$

$$u = 0, v = 0, T \to T_\infty at x = 0$$

$$u = U_0, v = 0, T \to T_\infty at y = 0 \tag{7}$$

$$u = 0, v = 0, T \to T_w at y \to \infty$$

Where x, y are Cartesian coordinate system. u, v are x, y component of flow velocity respectively is the local acceleration due to gravity ; υ is the kinematic viscosity; ρ is the density of the fluid ; κ is the thermal conductivity ; C_p is the specific heat at the constant pressure [7].

Since the solutions of the governing equations (4)-(5) under the initial (6) and boundary (7) conditions will be based on a finite difference method it is required to make the said equations dimensionless [14].

we attempt to solve the governing second order nonlinear coupled dimensionless partial differential equations with the associated initial and boundary conditions. For solving a transient free convection flow with heat and mass transfer past a semi infinite plate, *Callahan* and *Marner* (1976) used the difference method [15].

From the concept of the above discussion, for simplicity the explicit finite difference method has been used to solve equations continuity and momentum equation subject to the conditions . To obtain the difference equations the region of the flow is divided into a grid of lines parallel to X and Y axes where X -axes is taken along the plate and Y - axes is normal to the plate. Here we consider that the plate of height $X_{max} = 100$ i.e. X varies from 0 to 100 and regard $Y_{max} = 25$ as corresponding to $Y \to \infty$ i.e. Y varies 0 to 20. There are $m = 400$ and $n = 400$ grid spacing in the X and Y directions respectively as shown in the Fig. 2

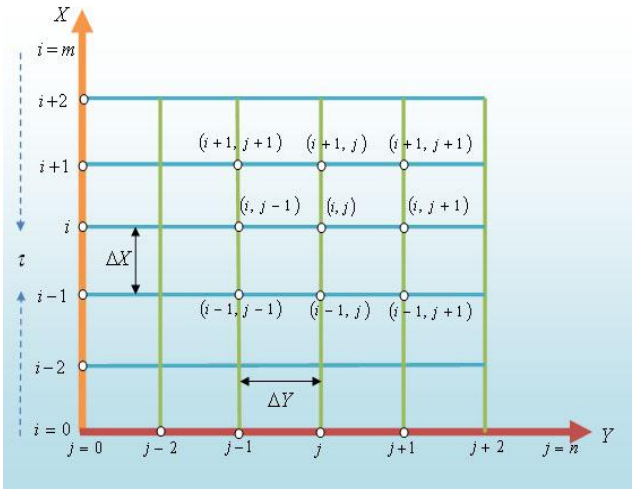

Fig. 2. The finite difference space grid

It is assumed that $\Delta X, \Delta Y$ are constant mesh sizes along X and Y directions respectively and taken as follows,

$$\Delta X = 0.5(0 \le x \le 200)$$
$$\Delta Y = 0.05(0 \le y \le 20)$$

With the smaller time step, $\Delta\tau = 0.001$.

2.2 Falkner equation

Let us consider the boundary layer equation of the type of potential flow for which similar solution exists. The boundary layer equation for two dimensional flow is [5]

$$u\frac{\partial u}{\partial x} + v\frac{\partial v}{\partial y} = U\frac{\partial U}{\partial x} + \nu\frac{\partial^2 u}{\partial y^2} \tag{8}$$

$$u\frac{\partial u}{\partial x} + v\frac{\partial v}{\partial y} = 0 \tag{9}$$

with boundary conditions

$$u = v = 0 \text{ at } y = 0 \tag{10}$$

$$\text{and } u = U(x) \text{ at } y \to \infty \tag{11}$$

by solving we get,

$$f''' + ff'' + \beta(1 - f'^2) = 0 \tag{12}$$

and the boundary conditions may be re-written as

$$f = 0, \quad f' = 0 \text{ at } \eta = 0$$
$$f' = 0 \quad \text{as } \eta \to \infty \tag{13}$$

Equation (12) with boundary conditions (13) was first deduced V.M. Falkner and S. W. Skan. So this equation is known as **Falknar-Skan Equation**

and solution of Falknar equation is $\therefore u = U\left[e^{-\xi} + \varepsilon\left[\left(\frac{1}{2} - \frac{1}{2}\beta + \xi\right)e^{-\xi} + \left(\frac{1}{2}\beta - \frac{1}{2}\right)e^{-2\xi}\right]\right]$.

2.3 Thermal boundary layer equation

Continuity equation $\frac{\partial u}{\partial x} + \frac{\partial v}{\partial y} = 0$ (14)

$$\text{Momentum equation}\ \frac{\partial u}{\partial t}+u\frac{\partial u}{\partial x}+v\frac{\partial u}{\partial y}=\upsilon\frac{\partial^2 u}{\partial y^2}+g\beta(T-T_\infty) \tag{15}$$

$$\text{Energy equation}\ \frac{\partial T}{\partial t}+u\frac{\partial T}{\partial x}+v\frac{\partial T}{\partial y}=\frac{\kappa}{\rho C_p}\frac{\partial^2 T}{\partial y^2}+\frac{\nu}{C_p}\left(\frac{\partial u}{\partial y}\right)^2 \tag{16}$$

With the corresponding initial and boundary conditions are

$$\text{At}\ \ t=0\ \ U=0, V=0 \text{ everywhere} \tag{17}$$

$t>0$
$u=0, v=0, T\to T_\infty \quad at\ x=0$

$$u=U_0, v=0, T\to T_\infty\ \ at\ y=0 \tag{18}$$

$u=0, v=0, T\to T_w \quad at\ y\to\infty$

Where x, y are Cartesian coordinate system. u, v are x, y component of flow velocity respectively is the local acceleration due to gravity ; υ is the kinematic viscosity; ρ is the density of the fluid ; κ is the thermal conductivity ; C_p is the specific heat at the constant pressure [11,16].

Since the solutions of the governing equations (14)-(16) under the initial (17) and boundary (18) conditions will be based on a finite difference method it is required to make the said equations dimensionless.

For this purpose we now introduce the following dimensionless variables;

$$X=\frac{xU_0}{\upsilon},\ Y=\frac{yU_0}{\upsilon},\ U=\frac{u}{U_0},\ V=\frac{v}{U_0},\ \tau=\frac{tU_0^2}{\upsilon},\ \bar{T}=\frac{T-T_\infty}{T_w-T_\infty}$$

Using these relations we have the following derivatives are

$$\frac{\partial u}{\partial t}=\frac{U_0{}^3}{\upsilon}\frac{\partial U}{\partial \tau},\quad \frac{\partial u}{\partial x}=\frac{U_0{}^2}{\upsilon}\frac{\partial U}{\partial X},\quad \frac{\partial u}{\partial y}=\frac{U_0{}^2}{\upsilon}\frac{\partial U}{\partial Y},$$

$$\frac{\partial^2 u}{\partial y^2}=\frac{U_0^3}{\upsilon^2}\frac{\partial^2 U}{\partial Y^2},\quad \frac{\partial v}{\partial y}=\frac{U_0^2}{\upsilon}\frac{\partial V}{\partial Y},$$

$$\frac{\partial T}{\partial x}=\frac{U_0\left(T_w-T_\infty\right)}{\upsilon}\frac{\partial \bar{T}}{\partial X};\ \frac{\partial T}{\partial y}=\frac{U_0\left(T_w-T_\infty\right)}{\upsilon}\frac{\partial \bar{T}}{\partial Y};$$

$$\frac{\partial^2 T}{\partial y^2}=\frac{U_0^2}{\nu^2}(T_w-T_\infty)\frac{\partial^2 \bar{T}}{\partial y^2}$$

Now we substitute the values of the above derivatives into the equations (14)-(16) and by simplifying we obtain the following nonlinear coupled partial differential equations in terms of dimensionless variables

$$\frac{\partial U}{\partial X}+\frac{\partial V}{\partial Y}=0 \tag{19}$$

$$\frac{\partial U}{\partial \tau}+U\frac{\partial U}{\partial X}+V\frac{\partial U}{\partial Y}=\frac{\partial^2 U}{\partial Y^2}+G_r\bar{T} \tag{20}$$

$$\frac{\partial \bar{T}}{\partial \tau}+U\frac{\partial \bar{T}}{\partial X}+V\frac{\partial \bar{T}}{\partial Y}=\frac{1}{P_r}\frac{\partial^2 \bar{T}}{\partial Y^2}+E_c\left(\frac{\partial U}{\partial Y}\right)^2 \tag{21}$$

Where,

$$\text{Grashof number} = G_r = \upsilon g\beta\frac{\left(T_w-T_\infty\right)}{U_0^{\,3}}$$

$$\text{Prandlt number} = \Pr = \frac{\upsilon\rho C_p}{K}$$

$$\text{Eckert number } E_c = \frac{U_0^2}{C_p}(T_w-T_\infty)$$

Also the associated initial and boundary conditions become

$$\tau = 0 \;\; U=0, V=0, \bar{T}=0 \text{ everywhere} \tag{22}$$

$$\tau > 0$$

$$U=0, V=0, \bar{T}=0 \; at \; X=0$$

$$U=0, V=0, \bar{T}=1 \; at \; Y=0 \tag{23}$$

$$U=0, V=0, \bar{T}=0 \; as \; Y\to\infty$$

3. Results and Discussion

3.1 Boundary layer equation and its solution

Our main purpose is to analysis the variation of stressing factor $\eta$and velocity f'. That means if we change the values of β and suction parameter f_w how the nature of velocity in terms of stressing factor will alter, that is it will increase or decrease, or it will remain constant.

In Figs. 3 to 4, we show that the velocity profile for different values of β at various suction parameter$f_w =$ 3,6,9 respectively. From these figures we conclude that the velocity profile decrease with the increase of suction parameter.

In Figs. 5 and 7 it is found that the velocity profile is increase with the increase of suction parameter for values of $\beta = 60,80$.

In Figs. 6 and 8 the velocity profile is decrease with the increase of suction parameter for values of $\beta = -60,-80$

In Figs. 9 to 10, it is said that the velocity profile are same for different values of $\beta(\pm)$ at the suction parameter $f_w = 3,6$

In Fig. 11 the velocity profile decreases with the increase of $\beta(+)$ and increases with the increase of $\beta(-)$ at $f_w = 9$

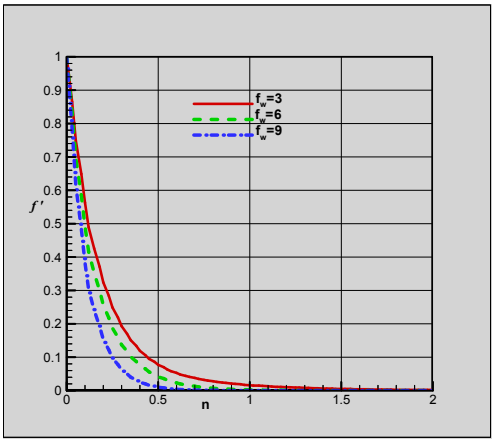

Fig. 3. For β=20 and $f_w = 3, 6, 9$

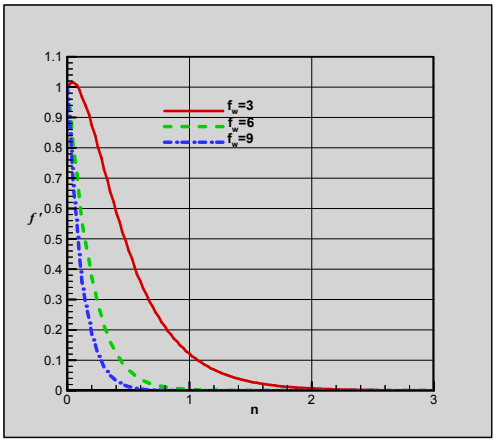

Fig. 4. For β=-20 and $f_w = 3, 6, 9$

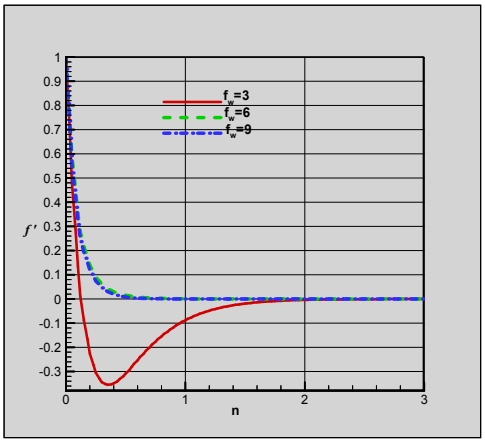

Fig. 5. For β=60 and $f_w = 3, 6, 9$

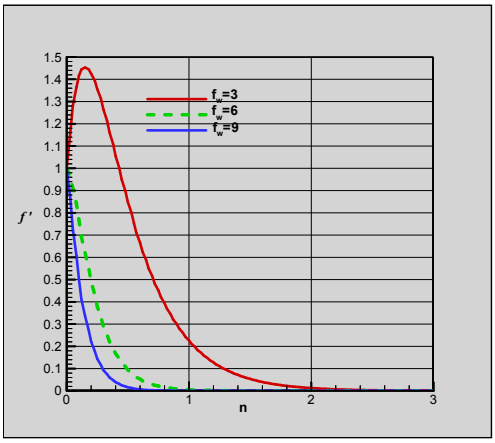

Fig. 6. For β=-60 and $f_w = 3, 6, 9$

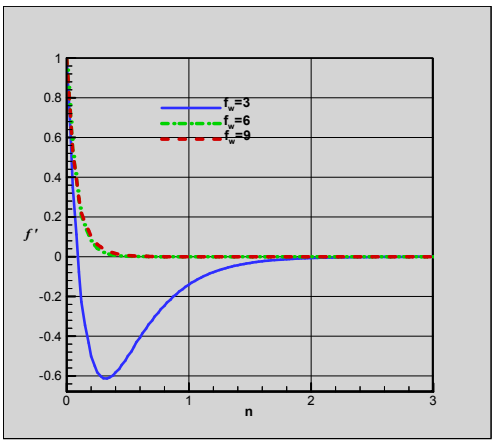

Fig. 7. For β=80 and $f_w = 3, 6, 9$

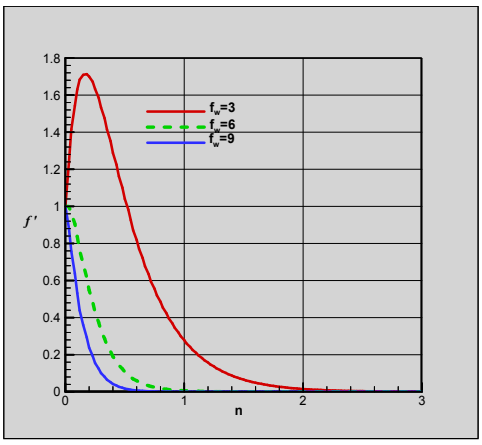

Fig. 8. For β=-80 and $f_w = 3, 6, 9$

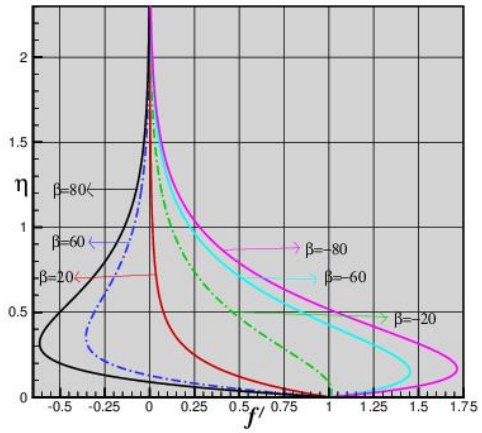

Fig. 9. For different values of β (±) at $f_w = 3$

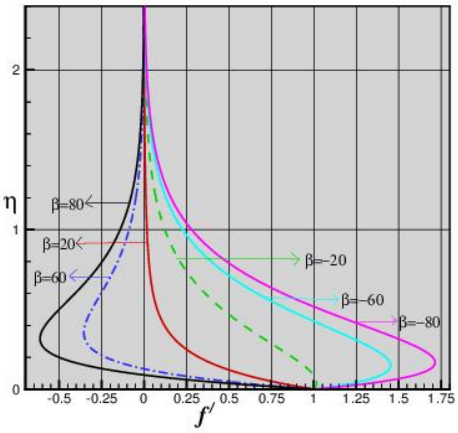

Fig. 10. For different values of β (±) at $f_w = 6$

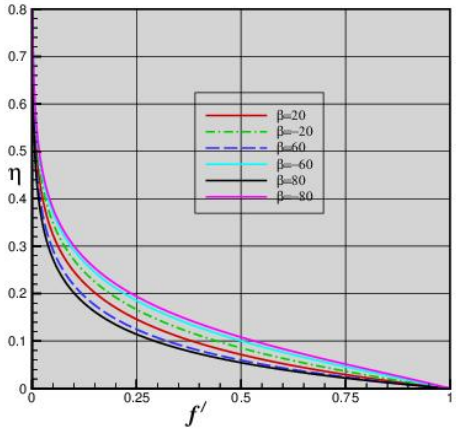

Fig. 11. For different values of β (±) at $f_w = 9$

3.2 Thermal boundary layer equation and its solution

The main goal of the computation is to obtain the steady state solutions for the non-dimensional velocity U and temperature T for different values of Prandtl P_r , Eckert E_c , and Grashof number Gr. For this purpose, computations have been carried out up to time τ =80. The results of the computations, however, show little changes in the above mentioned quantities after τ =50 have been reached. Thus the solution for τ =80 are essentially steady state solutions. Along with the steady state solutions the solutions for the transient values of U and T are shown in Fig. 12-22 for time τ =10, 50, respectively. The most important fluids are atmospheric air, water and saltwater. So the results are limited to P_r =0.71 (Prandtl number for air at 20^0C , P_r =7.0 (Prandtl number for air at 20^0C), and P_r =1.0 (Prandtl number for saltwater). The values of another parameter Eckert number is chosen arbitrarily. Fig. 11 to Fig. 14 shows the velocity profile for different values of Grashof number (Gr) at time τ =10,50. From these figure the velocity profile increase with the increase of Grashof number. Fig. 15 to 18 shows the velocity and temperature profile for different values of Prandtl number (Pr) at time τ =10,50. From these figure the velocity and temperature profile decrease with the increase of Prandtl number. Fig. 19 to Fig. 22 shows the velocity and temperature profile for different values of Eckert number (Ec)at time τ =10,50. From these figure the velocity and temperature profile increase with the increase of Eckert number(Ec).

In Fig. 11 to Fig 12, we show velocity profiles for different values of Gr at time $\tau = 10$ and $\tau = 50$ respectively. From these figures it is concluded that the velocity profile increases with the increase of Grashof number.

In Fig. 13 to Fig. 14 show the temperature profiles for different values of Gr at time $\tau = 10$ and $\tau = 50$ respectively. From these figures the temperature profiles decrease with the increase of Grashof number.

In Fig. 15 to Fig. 16 show the velocity profiles for different values of Pr at time $\tau = 10$ and $\tau = 50$ respectively. From these figures, we show that the velocity profile decrease with the increase of Prandtl number.

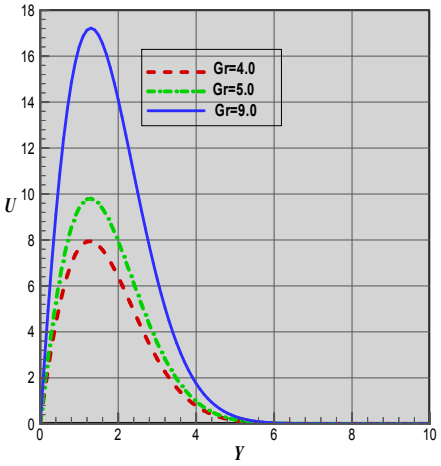

Fig. 11. Velocity profiles for different values of Grashof number when Pr=0.71 Ec=0.03 at time $\tau = 10$

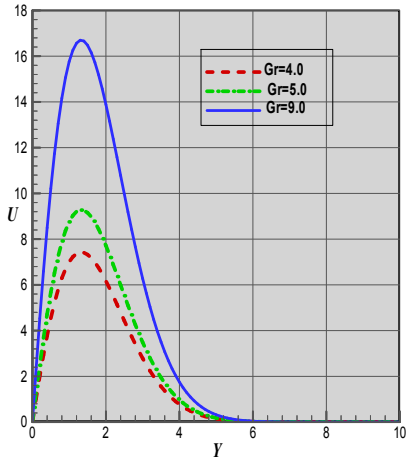

Fig. 12. Velocity profiles for different values of Grashof number when Pr=0.71 Ec=0.03 at time $\tau = 5\ 0$

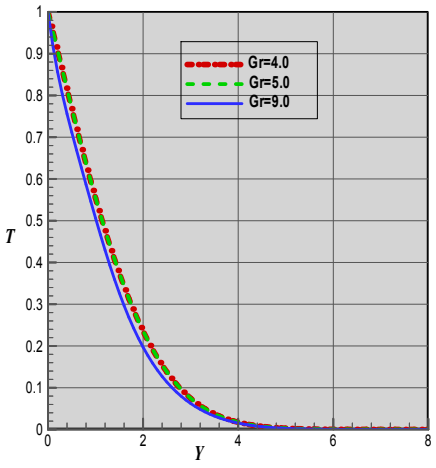

Fig. 13. Temperature profile for different values of Grashof number when Pr=0.71, Ec=0.03 at time $\tau = 10$

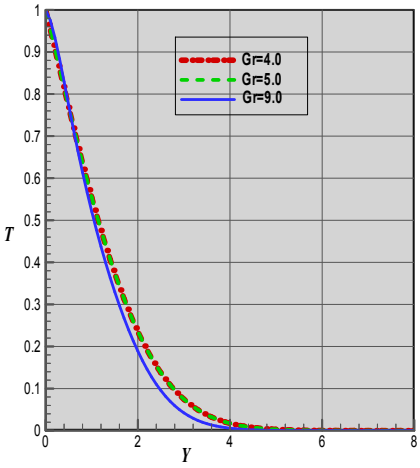

Fig. 14. Temperature profile for different values of Grashof number when Pr=0.71, Ec=0.03 at time $\tau = 5\ 0$

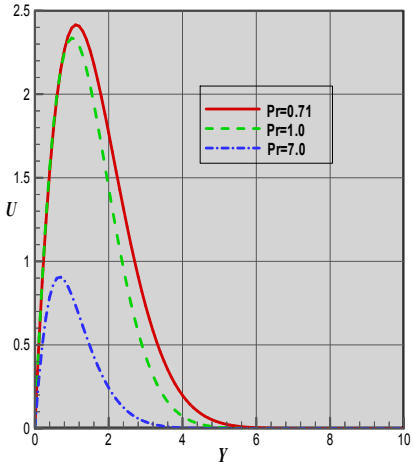

Fig. 15. Velocity profiles for different values of Prandtl number when Gr=4 Ec=0.01 at time $\tau = 10$

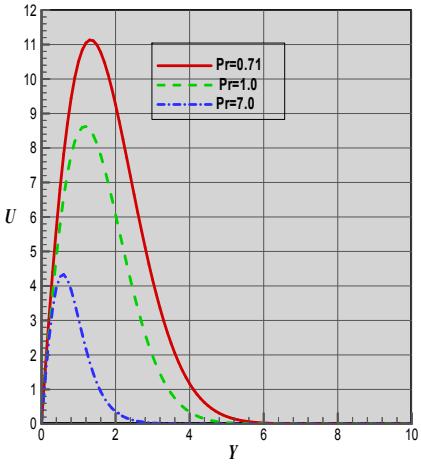

Fig. 16. Velocity profiles for different values of Prandtl number when Gr=4 Ec=0.01 at time $\tau = 50$

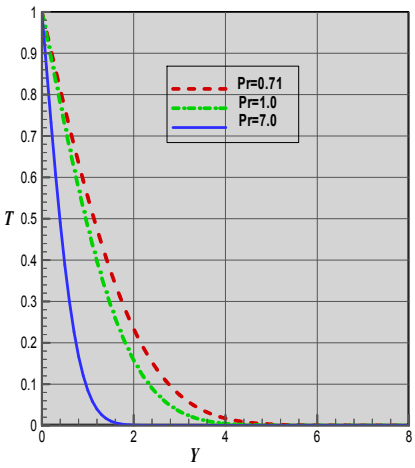

Fig.17. Temperature profile for different values of Prandtl number when Gr=4, Ec=0.01 at time $\tau = 10$

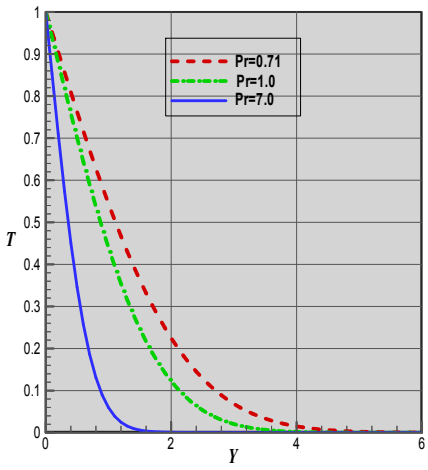

Fig. 18. Temperature profile for different values of Prandtl number when Gr=4, Ec=0.01 at time $\tau = 50$

In Fig. 17 to Fig. 18 show the temperature profiles for different values of Pr at time $\tau = 10$ and $\tau = 50$ respectively. From these figures the temperature profile decreases with the increase of Prandtl number.

In Fig. 19 to Fig 20 show the velocity profiles for different values of Ec at time $\tau = 10$ and $\tau = 50$ respectively. From these figures it is found that the velocity profile increase with the increase of Eckert number.

In Fig. 21 to Fig 22 show the temperature profiles for different values of Ec at time $\tau = 10$ and $\tau = 50$ respectively. From these figures the temperature profiles increase with the increase of Eckert number.

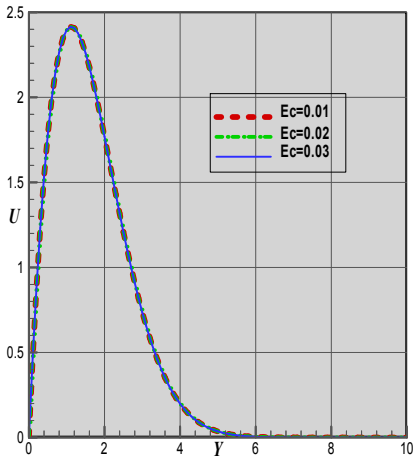

Fig. 19. Velocity profiles for different Values of Eckert number when Gr=4 Pr=0.71 at time $\tau = 10$

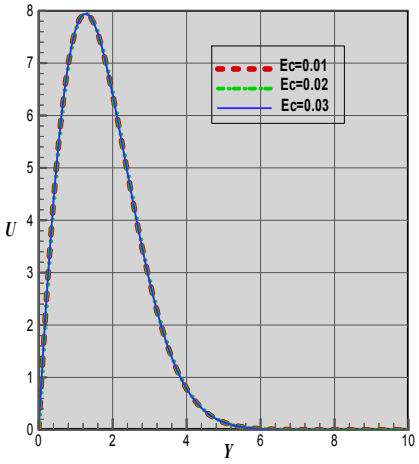

Fig. 20. Velocity profiles for different values of Eckert number when Gr=4 Pr=0.71 at time $\tau = 50$

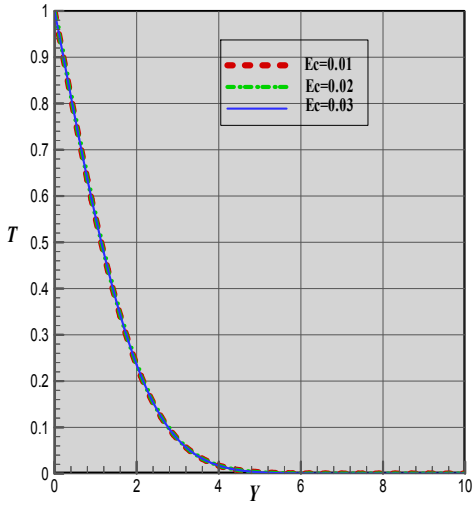

Fig. 21. Temperature profile for different values of Eckert number when Gr=4, Pr=0.71 at time $\tau = 10$

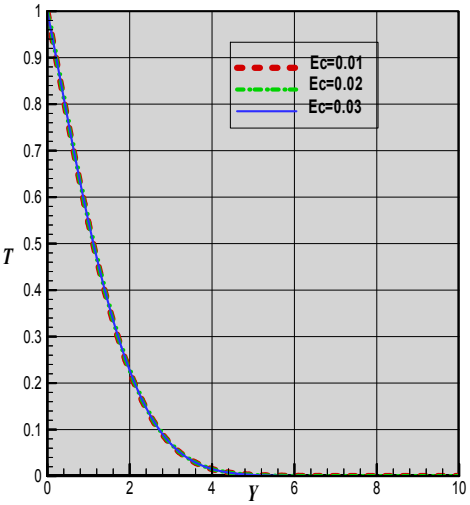

Fig. 22. Temperature profile for different values of Eckert number when Gr=4, Pr=0.71 at time $\tau = 50$

4 Conclusion

The Thermal Boundary Layer Equation had been derived from Navier-stoke and concentration equation by boundary layer technique. Boundary Layer equation has been non-dimensionalised by using non-dimensional variable. The non-dimensional boundary layer equations are non-linear partial differential

equations. These equations are solved by finite difference method. Finite difference solution of heat and mass transfer flow is studied to examine the velocity and temperature. The effect on the velocity and temperature for the various important parameters entering into the problems are separately discussed into the problem with the help of graphs. Then the results in the form of velocity and temperature distribution are shown graphically.

Competing Interests

Authors have declared that no competing interests exist.

References

[1] Makanga Robert Ayiecha. August 2017, ISSN-2410-1397, The numerical solution for laminar boundary layer flow over a flat plate, university of Nairobi.

[2] Swarep, Shanti. Hydrodynamics (5th edition). Krishna prakashan Media (p). Ltd. Pijush, K. K and Cohen M. Ira, Fluid Mechanics (second edition). 2005;323-330.

[3] Modi PN, Seth SM. Hydrodynamics and Fluid mechanics (Thirteenth edition); 2000.

[4] Ullah H, Islam S, Idrees M, Arif M. August 2013, Solution of Boundary Layer Problems with Heat Transfer by Optimal Homotopy Asymptotic Method, Hindawi Publishing Corporation. Volume 2013, Article ID 324869, 10 pages.

[5] Krishnendu Bhattacharyya M, Uddin S, Layek GC. 21 April 2016, Exact solution for thermal boundary layer in Casson fluid flow over permeable shrinking sheet with variable wall temperature and thermal radiation, Alexandria Engineering Journal. 2016;55:1703–1712.

[6] Rashidi MM, Vishnu Ganesh N, Abdul Hakeem AK, Ganga B. Buoyancy effect on MHD flow of nanofluid over a stretching sheet in the presence of thermal radiation. Journal of Molecular Liquids. 2014;198:234–238.

[7] Raisinghanisa MD. Fluid dynamics with hydrodynamics (Art. 15.2). S. Chand & Company Ltd; 2002.

[8] Thomson Milne LM. Theoretical Hydrodynamics Fifth edition; 1968.

[9] Yaun SW. Foundations of fluid mechanics. Prentice-Hall of India Private Limited; 1967.

[10] Rahim Shah, Tongxing Li. The thermal and laminar boundary layer flow over prolate and oblate spheroids. International Journal of Heat and Mass Transfer. 2018;121:607–619.

[11] Bansal JL. Viscous fluid dynamics (Second Edition). Oxford & IBH publishing CO.PVT.LTD; 2004.

[12] Garrett SJ, Hussain Z, Stephen SO. Boundary-layer transition on broad cones rotating in an imposed axial flow. AIAA J. 2010;48:1184–1194.

[13] Rosales M, Valencia A. A note on solution of blasius equation by Fourier series. Advances in Applied Mechanics. 2009;6:33–38.

[14] Rajput KR, Chand S. Heat and mass transfer (Multicolour edition). S. Chand & Company Ltd. 2007;373-387.

[15] Pratap, Rudra A quick introduction for scientists and engineers. Oxford University Press; 2006.

[16] Harman, Schlichting. Dr. Boundary Layer theory (6th Edition). McGraw-Hill Company.

Peer-review history:
The peer review history for this paper can be accessed here (Please copy paste the total link in your browser address bar)
http://www.sciencedomain.org/review-history/27853